



## Improving the P-wave Velocity Determination by Considering the Effects of Joint Properties in Artificial Rock Samples

Mohammad Rezaei<sup>1\*</sup>, Seyed Pourya Hosseini<sup>1</sup>, Danial Jahed Armaghani<sup>2</sup>, and Manoj Khandelwal<sup>3</sup>

1. Department of Mining Engineering, Faculty of Engineering, University of Kurdistan, Sanandaj, Iran

2. School of Civil and Environmental Engineering, University of Technology Sydney, Ultimo, NSW 2007, Australia

3. Institute of Innovation, Science and Sustainability, Federation University Australia, Ballarat, VIC 3350, Australia

### Article Info

Received 24 October 2024

Received in Revised form 14 November 2024

Accepted 19 December 2024

Published online 19 December 2024

DOI: [10.22044/jme.2024.15261.2924](https://doi.org/10.22044/jme.2024.15261.2924)

### Keywords

Rock mass

Joint

Longitudinal wave velocity

Experimental study

Statistical analysis

### Abstract

This paper presents an experimental-statistical study investigating the influence of five joint properties: density, filling type, angle, aperture, and roughness on the longitudinal wave velocity (LWV) of concrete samples. To achieve this, each of the five properties is categorized into distinct groups with specific intervals. Concrete samples measuring 15×15×15 cm are prepared in the laboratory based on an optimal combination of 75% sand, 15% cement, and 10% water. The LWV values of these samples are then measured. The experimental results indicate that joint density, roughness, and aperture have an inverse relation with LWV, resulting in reductions of 82%, 22.5% and 49%, respectively. Additionally, an approximate sinusoidal relationship between LWV and joint angle is established, leading to a variation of approximately 10% in LWV values for different joint angles. To evaluate the effect of joint filling on LWV, various filling materials, including iron oxide, calcite, silica, clay, and gypsum are used, resulting in approximately a 34% variation in LWV values. It was found that gypsum filling yields the highest LWV value while iron oxide filling produces the lowest. Furthermore, analysis of variance (ANOVA) confirms that a polynomial quadratic equation best represents the relation between LWV and each of the joint characteristics, with determination coefficient (R<sup>2</sup>) values ranging from 0.694 to 0.99. Finally, a verification study using "validation samples" demonstrates the acceptable accuracy for the proposed equations, with minimum relative errors ranging from 3% to 13%, a low root mean square error of 189.08 m/s, and a high R<sup>2</sup> value of 0.926. This research enhances understanding of wave propagation through jointed rock masses with varying joint characteristics and provides theoretical support for rock reorganization and dynamic stability analysis of rock masses.

## 1. Introduction

Obtaining accurate information about the status of rock mass is crucial for designing geotechnical projects. A primary step in developing rock mechanics and civil engineering designs involves determining the deformability and strength of jointed rock masses. Consequently, understanding the properties of intact rock and its existing discontinuities is essential for comprehending rock mass behavior. The wave velocity through the rock is a key parameter influenced by both the properties of intact rock and the discontinuities within the rock mass. The main discontinuities

typically include joints, bedding surfaces and faults. The key properties of joints can be categorized into three categories: geometrical properties, characteristics of joint surfaces, and types of filling material. Important geometrical features include aperture, density and angle, while joint surface properties encompass factors such as wall strength, roughness and weathering [1–4].

Acquiring detailed information about the joints and discontinuities within a rock mass enables engineers to accurately assess its overall condition. Therefore, it is vital to thoroughly understand joint

✉ Corresponding author: [m.rezaei@uok.ac.ir](mailto:m.rezaei@uok.ac.ir) (M. Rezaei)

characteristics and their impacts on other rock mass properties to get precise insight into the system. Joints significantly influence the physical, hydrogeological, and mechanical properties of the rock mass, contributing to its complexity. This complexity increases when dynamic forces—such as those from earthquake or blasting—interact with rock, leading to wave propagation. The propagation of waves through a jointed rock mass depends on both the type of rock and the properties of its joints. For instance, when a wave encounters a joint interface, part of it is reflected while another portion slows down with some absorption, resulting in wave attenuation. This process alters both the wave distribution pattern and transit time. Given these factors' significance, extensive research has focused on how joint characteristics affect wave behavior and propagation patterns across various geoscientific structures [5–7].

There are three primary methods in the literature for studying and analyzing wave propagation in jointed rock masses: theoretical [8–16], experimental [7, 10, 17–27], and numerical [7, 19, 23, 28–31] models. Theoretical approaches typically rely on approximations [8–10, 12, 13], displacement discontinuity methods [11, 14], and equivalent [15, 16] models. Various experimental investigations have been conducted to understand wave propagation in jointed rock masses, employing common testing methods such as resonant-based experiments [19, 21, 22], bender-based tests [24], Hopkinson-based tests [17, 26, 27], and wave velocity-based experiments [7, 21–23, 28]. The most widely used numerical model for analyzing wave propagation in jointed rock masses is the discrete element method, which is implemented through various computational codes [7, 13, 28–31].

Numerous researchers have examined the impact of joint properties, such as joint density, on LWV in different types of rocks [7, 23, 32–36]. They consistently found an inverse relationship between LWV and joint density. Additionally, previous studies demonstrated that increasing joint roughness leads to a reduction in LWV [7, 22, 23, 37, 38]. Some researchers observed an approximate sinusoidal relationship between LWV and joint angle [34, 39]. Varma et al. [7] concluded that as the joint angle increased from  $0^\circ$  to  $10^\circ$ , LWV decreased, remains constant between  $10^\circ$  and  $50^\circ$ , but increased again as the angle rose from  $50^\circ$  to  $70^\circ$ . The influence of joint thickness on LWV was studied by Huang et al. [40] and Yang et al. [41], who found that LWV decreases as joint thickness increases.

Abbas et al. [42] conducted a laboratory study on a composite rock consisting of sandstone-shale-sandstone layers with various joints at different angles to assess the anisotropic behavior of body wave velocities. They found that the LWV decreased by 35% as the joint orientation angles increased from  $30^\circ$  to  $90^\circ$ . In a separate study, Fan et al. [43] employed a theoretical model to investigate the propagation and attenuation of LWV in jointed rock masses, considering both single and multiple parallel joints. Their findings indicated that as the number of joints increased, the magnitude of LWV decreased. Tartoussi et al. [44] examined the effect of filled discontinuities with varying widths, lengths, and infilling material densities on LWV, concluding that changes in velocity were more closely related to the width of the discontinuities than to amplitude attenuation. Yang et al. [45] conducted a laboratory investigation into the interaction between clay minerals and water saturation in filled rock joints, revealing inconsistent results regarding the impact of water saturation due to the hydration of the clay materials. Hu et al. [46] utilized numerical modeling to study LWV propagation across jointed rock masses with both single and multiple joints. Lastly, Kaixing et al. [47] explored the effect of block fractures on LWV propagation, demonstrating that LWV decreases as block fractures increase.

In the majority of these studies, the focus on wave propagation was primarily limited to seismic factors, while aspects such as wave transmission, reflectance factors, and the influence of joint characteristics were largely overlooked. Furthermore, previous research mainly examined the direct or inverse relationship between LWV and individual joint properties without exploring their optimal interrelationships. By thoroughly characterizing joints and determining ultrasonic wave velocity through rock masses, researchers can gain deeper insights into rock mass quality and key mechanical characteristics. In light of these gaps, the current research investigates the propagation of LWV in artificial jointed rock samples, considering the effect of joint roughness, density, aperture, angle, and filling type. The research methods involve the preparation of artificial samples, comprehensive experimental testing on these specimens, and statistical analyses to establish optimal relationships between LWV and joint properties. The primary novelty of this study lies in utilizing laboratory-derived LWV and joint characteristics datasets, contrasting with the indirect seismic data used in most previous studies.

Additionally, this research examines the effect of all relevant joint properties on LWV and proposes predictive optimal relationships for determining LWV, facilitating rapid and cost-effective assessments.

## 2. Experimental study

### 2.1. Sample preparation

In this study, a sufficient number of artificial specimens were prepared for experimental analysis. To create these artificial samples, plastic molds measuring  $15\text{ cm} \times 15\text{ cm} \times 15\text{ cm}$  were used (Figure 1a). The utilization of artificial samples is a common practice in rock engineering, primarily due to the challenges associated with obtaining natural rock samples that possess the desired joint characteristics [7, 15, 18, 48, 49]. It is essential to use homogeneous and isotropic materials when preparing suitable artificial specimens and conducting accurate tests to obtain precise results. Additionally, the design of the specimen components must ensure that the samples exhibit high strength and facilitate the creation of artificial joints within their structure. In this research, an optimal mix of sand, type II cement, and water was employed to prepare the artificial specimens, owing to its high strength, good joint flexibility,

accessibility of materials, and ease of placement in molds.

Generally, the materials used to fabricate artificial rock samples include gravel, sand, cement, and water. To prepare these samples, a 30-mesh sieve was first used to remove impurities from the materials. The mixture was then prepared according to an optimal ratio of 75% sand, 15% cement, and 10% water. This composition yielded a mean unconfined compressive strength approximately  $40 \pm 2$  MPa, achieved through a trial-and-error method. After thorough mixing, a homogeneous mortar was created and transferred into the plastic molds. Prior to filling, the inner surfaces of the molds were lubricated with grease to prevent the mortar from adhering and to ensure easy removal of the samples (Figure 1). To achieve the intended joint characteristics, greased iron sheets were placed between the layers in the samples (Figure 1 b). Once the mortar was placed into the molds, the samples were positioned on a shaking table for one minute to eliminate air bubbles within the mortar. After two days, the molds were removed, and the samples were allowed to cure at room temperature for 28 days to reach their final strength before conducting LWV tests. A prepared sample with dimensions of  $15 \times 15 \times 15\text{ cm}$  is presented in Figure 1c.

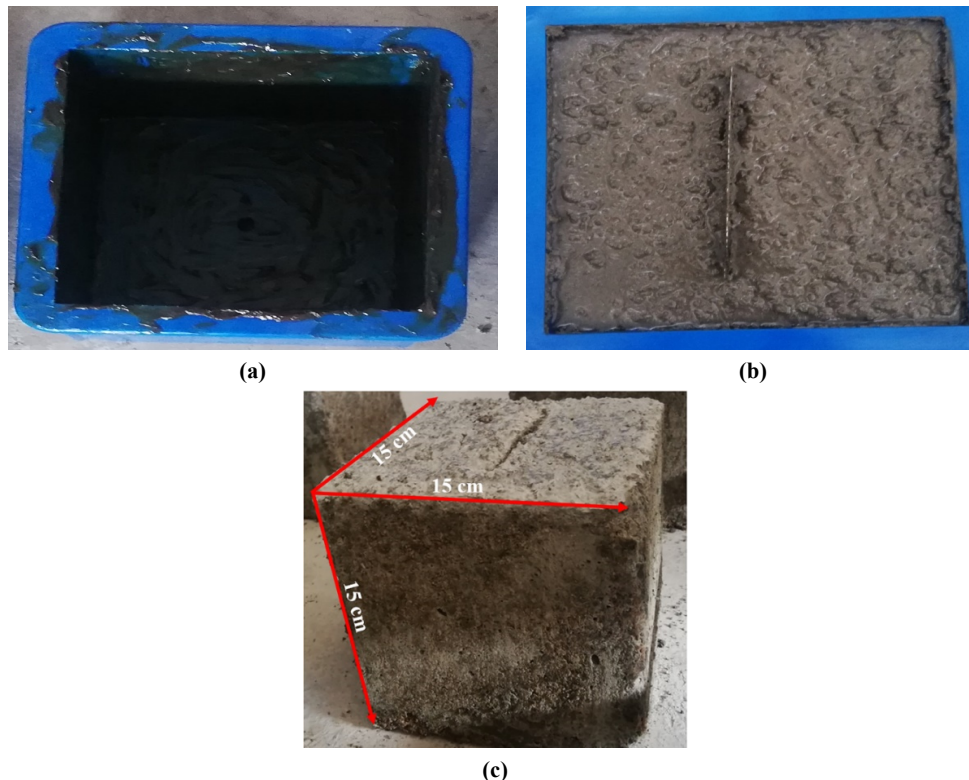
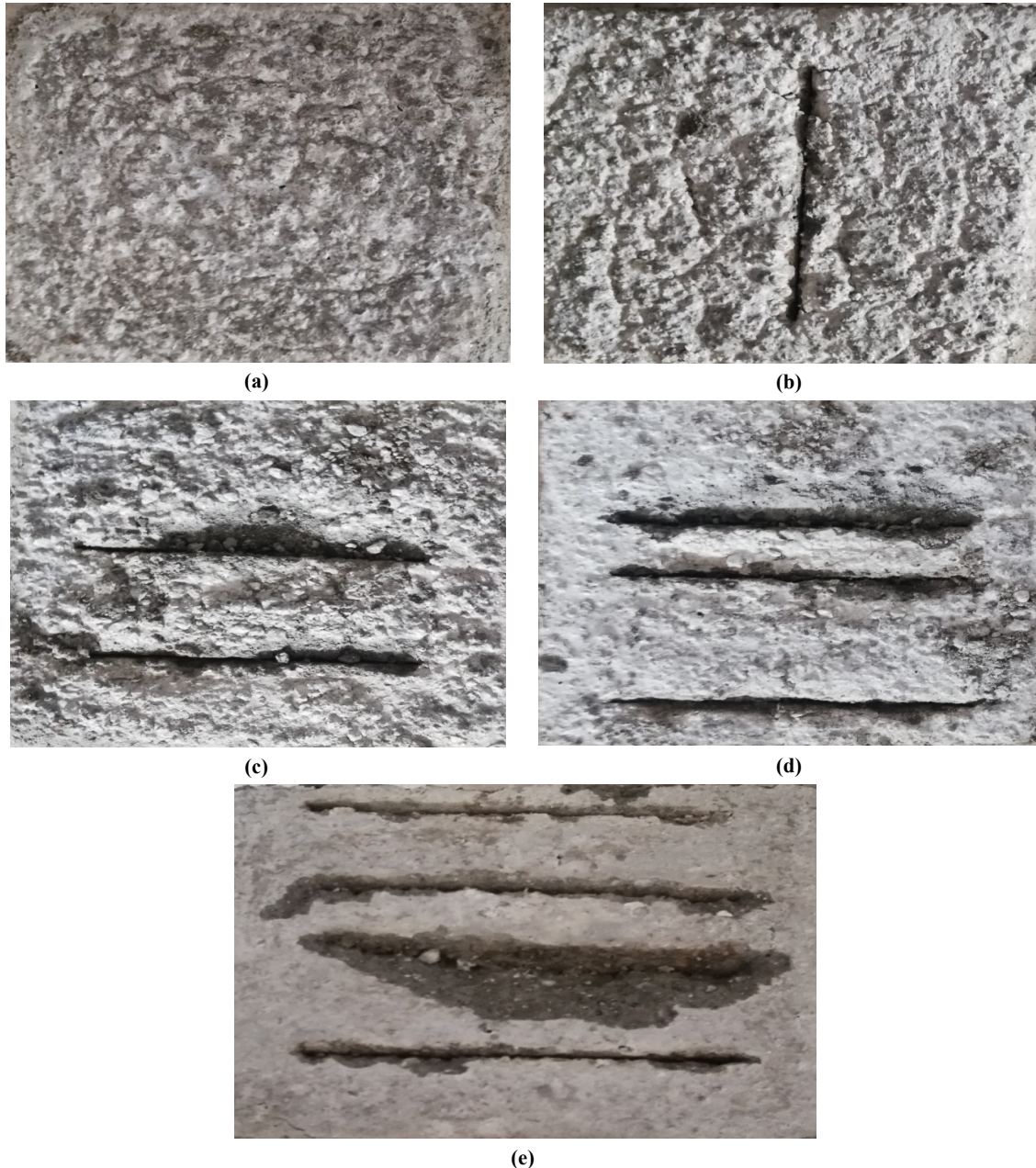


Figure 1. a) Used plastic molds for sample preparation, with lubrication of their inner surfaces using grease, b) Placement of the mortar and iron sheet into the plastic molds, c) A prepared sample with dimensions of  $15\text{ cm} \times 15\text{ cm} \times 15\text{ cm}$ .

The primary parameters examined in this study include joint density, joint filling, joint angle, joint aperture, and joint roughness. To assess the effect of joint density on LWV, five artificial samples were cast in the laboratory. These samples

represent different configurations: zero (no joints), one joint, two joints, three joints, and four joints. The prepared artificial samples, considering the joint density parameter, are shown in Figure 2.



**Figure 2.** Prepared concrete samples with varying joint configurations: a) Zero joint (no joints), b) One joint, c) Two joints, d) Three joints, e) Four joints.

The filling materials within the joints significantly influence the engineering behavior of rock mass. To study the effect of different filling types on LWV, natural materials—namely iron oxide, calcite, silica, clay, and gypsum—were used

as the joint fillers. After preparing the samples and creating the joints, the fillers were applied and maintained for 14 days. The constructed samples with various filling materials are illustrated in Figure 3.

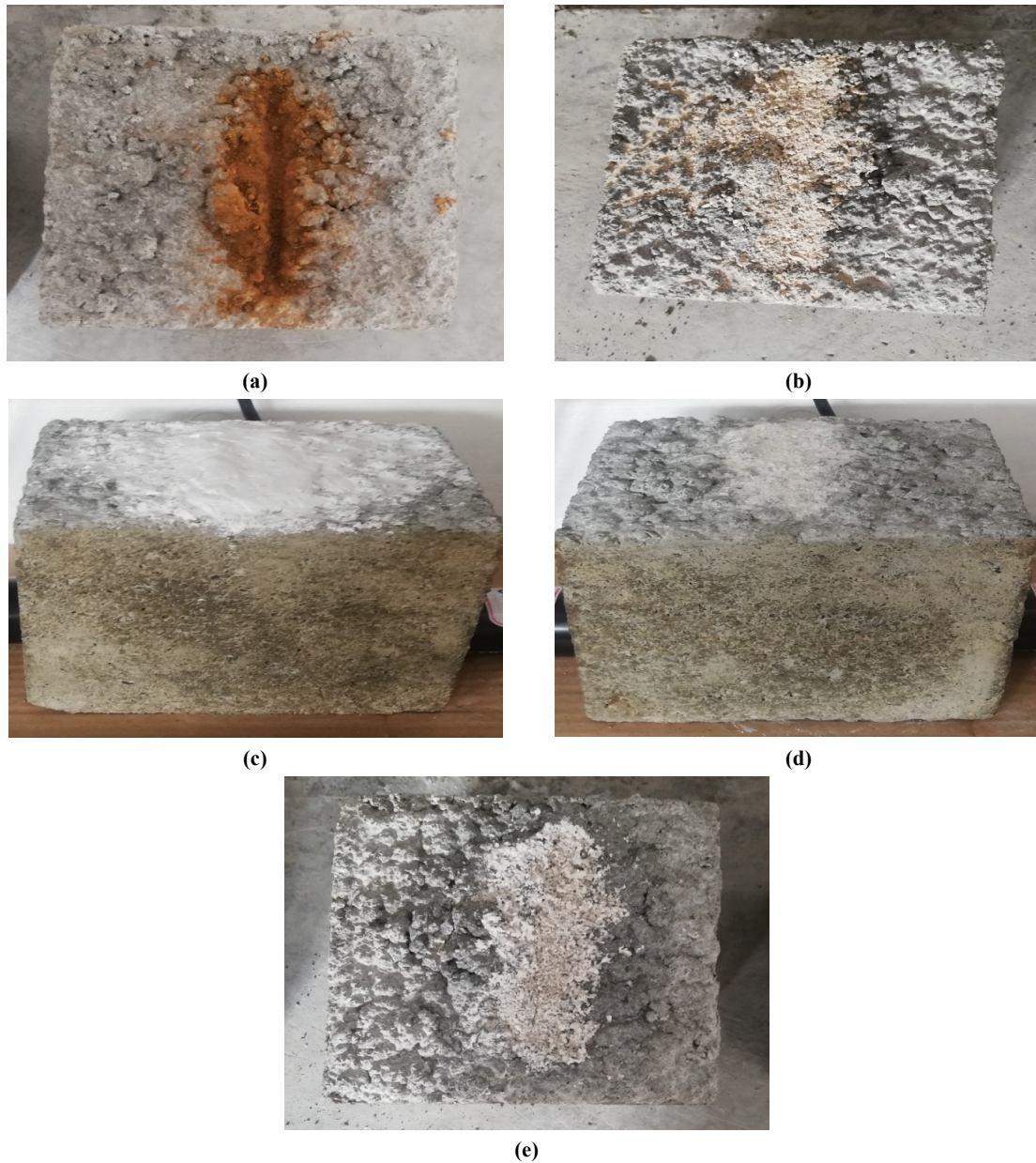


**Figure 3. Prepared concrete samples with different fillings: a) Iron oxide, b) Clay, c) Gypsum, d) Calcite, e) Silica.**

Joint angle is another parameter that affects LWV. Four artificial specimens were utilized to test the effect of joint angle on LWV. Following established experimental methods, mortar was poured into the molds, after which iron sheets were inserted into the mortar. A graduated protractor was employed to align the iron sheets at specific angles to create artificial joints at various orientations. After two days, the iron sheets were removed from the mortar, and the samples were extracted from the plastic molds two days later. This approach yielded four different samples with

joint angles of  $30^{\circ}$ ,  $45^{\circ}$ ,  $60^{\circ}$ , and  $90^{\circ}$  as depicted in Figure 4.

Joint aperture is a key parameter influencing wave velocity through rock masses. In nature, joints with varying apertures can significantly affect wave velocity within rock formations. This study examines the effect of joint aperture on LWV. To create different aperture sizes, iron sheets with thicknesses of 0.5 mm, 1 mm, 1.5 mm, and 2 mm were used to form four samples with the desired apertures, following the aforementioned sample preparation process. The prepared samples are shown in Figure 5.

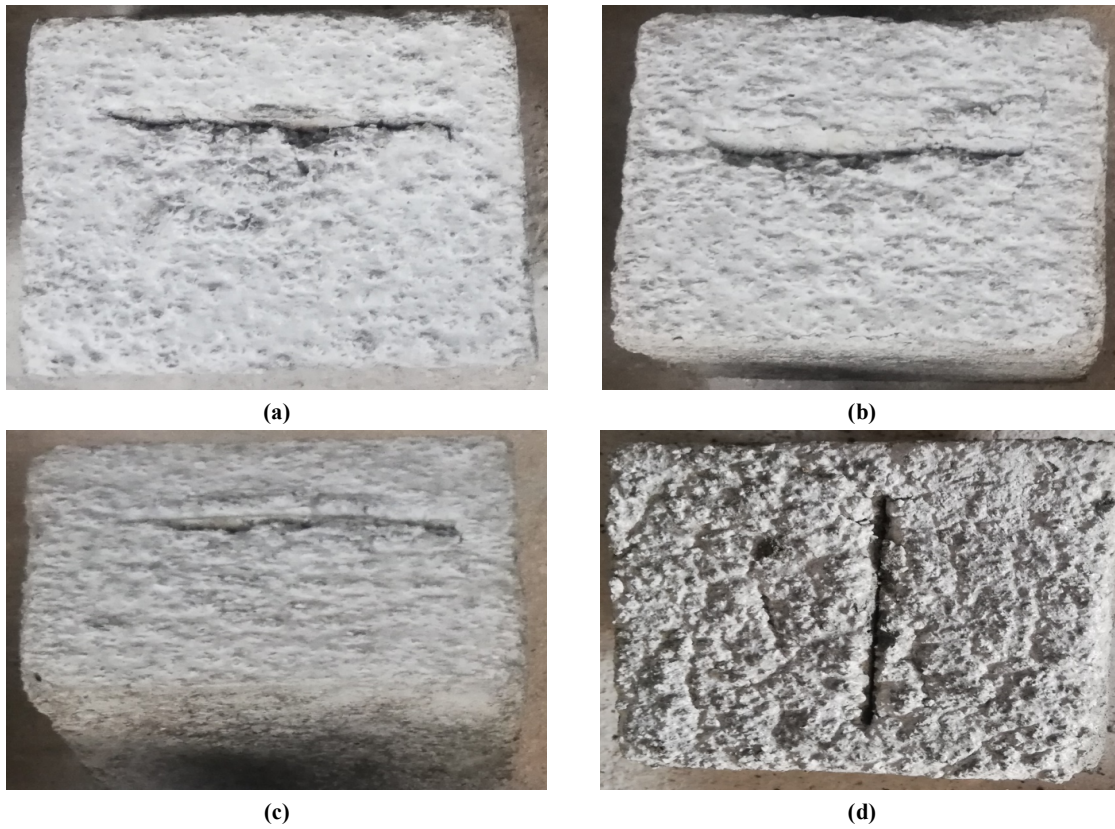


Figure 4. Prepared concrete samples with varying joint angles: a) Angle of 30°, b) Angle of 45°, c) Angle of 60°, d) Angle of 90°.

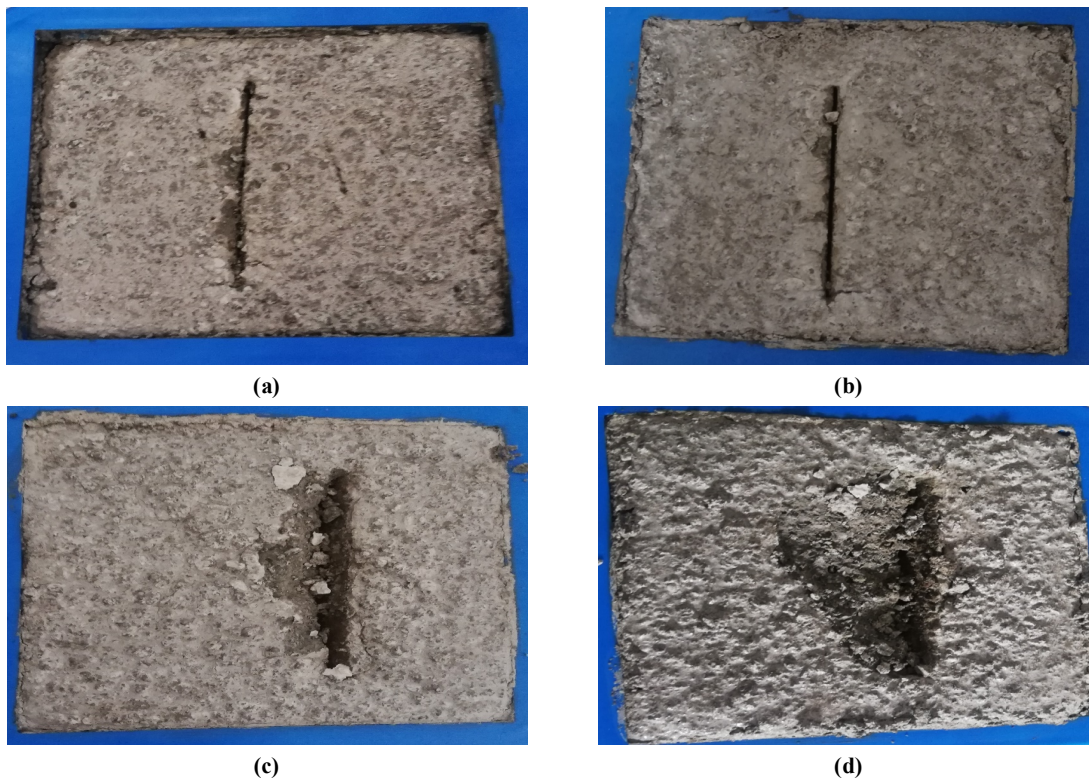
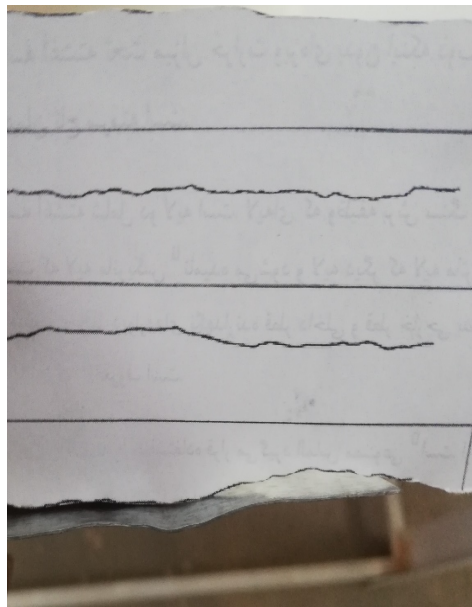


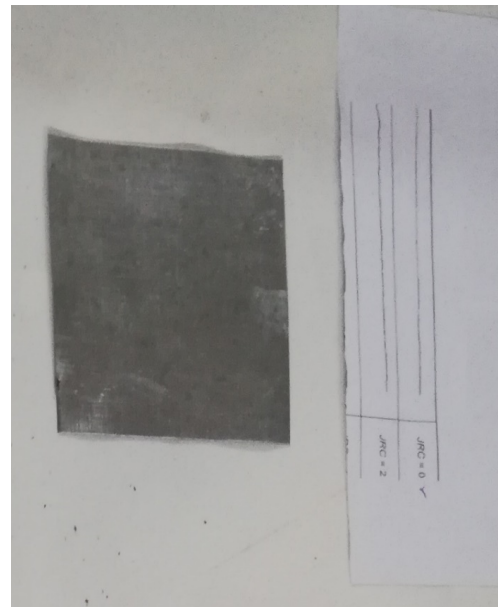
Figure 5. Prepared concrete samples with varying joint apertures: a) Joint aperture of 0.5 mm, b) Joint aperture of 1 mm, c) Joint aperture of 1.5 mm, d) Joint aperture of 2 mm.

In natural rock formations, joint roughness significantly influences both the physical and mechanical properties of the rock. Roughness is a crucial characteristic of joints that affects ultrasonic wave velocity through rock masses. Variations in joint roughness can lead to changes in ultrasonic wave velocity. Following Barton's standard profile [50], four samples with differing degrees of roughness were created. A smooth iron sheet was utilized to achieve a joint roughness coefficient (JRC) value of 0-2. For joints with rougher textures, JRC values of 4-6, 10-12, and 14-

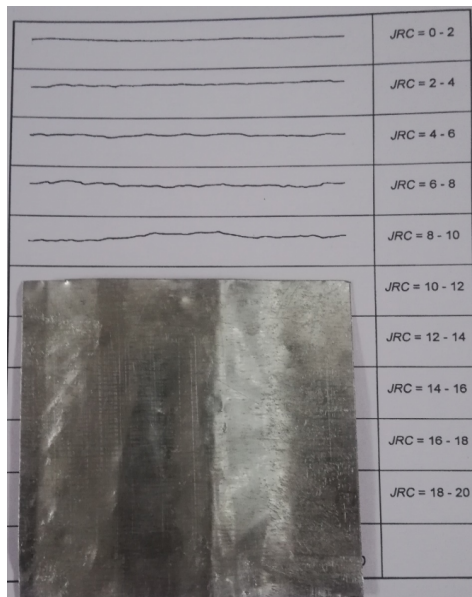
16 were produced using manually designed profiles based on Barton's standard. The iron sheets were made flexible to ensure that their surfaces conformed to Barton's standard profile, facilitating the creation of joints with the desired roughness in the mortar. The manually created profiles, along with the prepared rough sheets for joints with JRC values of 4-6, 10-12, and 14-16, are illustrated in Figure 6. Additionally, a sample featuring joints with JRC values of 0-2, 4-6, 10-12, and 14-16 is presented in Figure 7.



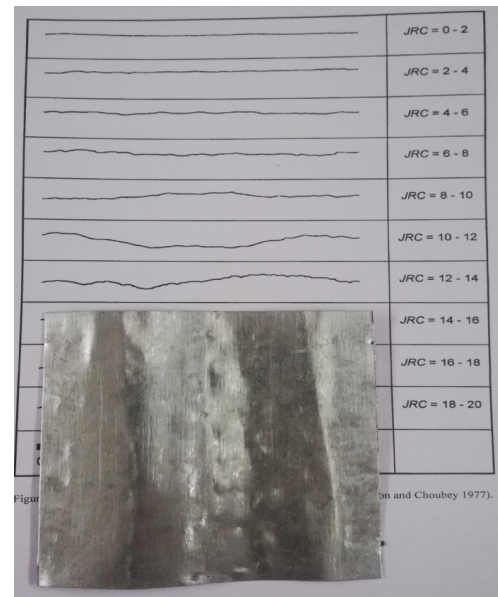
(a)



(b)



(c)



(d)

Figure 6. a) Manually constructed profile for inducing joint roughness, b) Iron sheet for creating JRC=4-6, c) Iron sheet for creating JRC=10-12, d) Iron sheet for creating JRC=14-16.

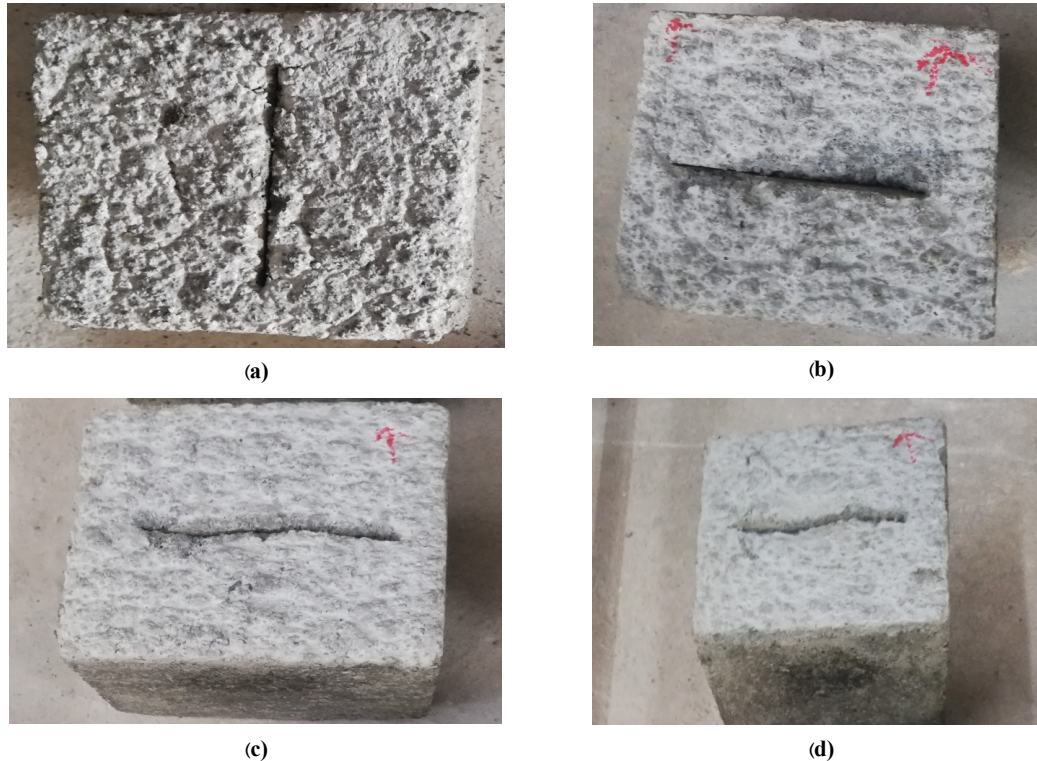


**Figure 7. Prepared concrete samples with varying joint roughness: a) Sample with JRC=0-2, b) Sample with JRC=4-6, c) Sample with JRC=10-12, d) Sample with JRC=14-16.**

In the subsequent section, empirical relationships between joint properties and LWV are proposed. To test and validate each proposed equation, two separate samples were prepared, referred to as "validation samples". Specifically, two samples with joint densities of 5 and 6, two samples with joint angles of  $15^\circ$  and  $75^\circ$ , two samples with joint aperture of 2.5 mm and 3 mm, and two samples with JRC of 8-10 and 18-20 were constructed. The samples shown in Figures 2–5 and 7 will be used to develop new equations relating joint properties to LWV, while the "validation samples" will be employed to validate these proposed equations.

## 2.2. LWV test

As mentioned in the introduction, the ultrasonic wave velocity testing technique has been extensively used in previous studies to analyze wave propagation patterns in various rock types [51–57]. In the LWV test, a sinusoidal wave of moderate frequency is generated at one end of the sample, propagates through it, and is detected at the opposite end. The LWV of the prepared samples is measured using the PUNDIT device (Figure 8a) following the ISRM standard method [58]. This

instrument consists of two transducers operating at a wave frequency of 54 kHz, a pulse maker, two connection cables, a calibration rod designed for a travel time of  $25.4 \mu\text{s}$ , and an electronic calculator that measures travel times with an accuracy of  $0.1 \mu\text{s}$ . To measure LWV, a pulse is emitted by one transducer, travels through the sample, and is received by the other transducer. The measurement procedure for assessing LWV in an artificially prepared sample is illustrated in Figure 8b. The LWV value is calculated by dividing the sample length (measured manually) by the transmission time (measured by the PUNDIT device). The measured LWV values vary based on different parameters: they range from 480 to 2720 m/s for varying densities, from 1620 to 2460 m/s for different fillings, from 1840 to 2050 m/s for varying angles, from 1045 to 2050 m/s for different apertures, and from 1590 to 2050 m/s for varying JRCs. In contrast, the LWV values for the "validation samples" are recorded as 470 and 450 m/s for joint densities of 5 and 6, respectively; 2100 and 1850 m/s for joint angles of  $15^\circ$  and  $75^\circ$ ; 650 and 450 m/s for joints with apertures of 2.5 and 3 mm; and 1650 and 1460 m/s for JRC values of 8-10 and 18-20, respectively.

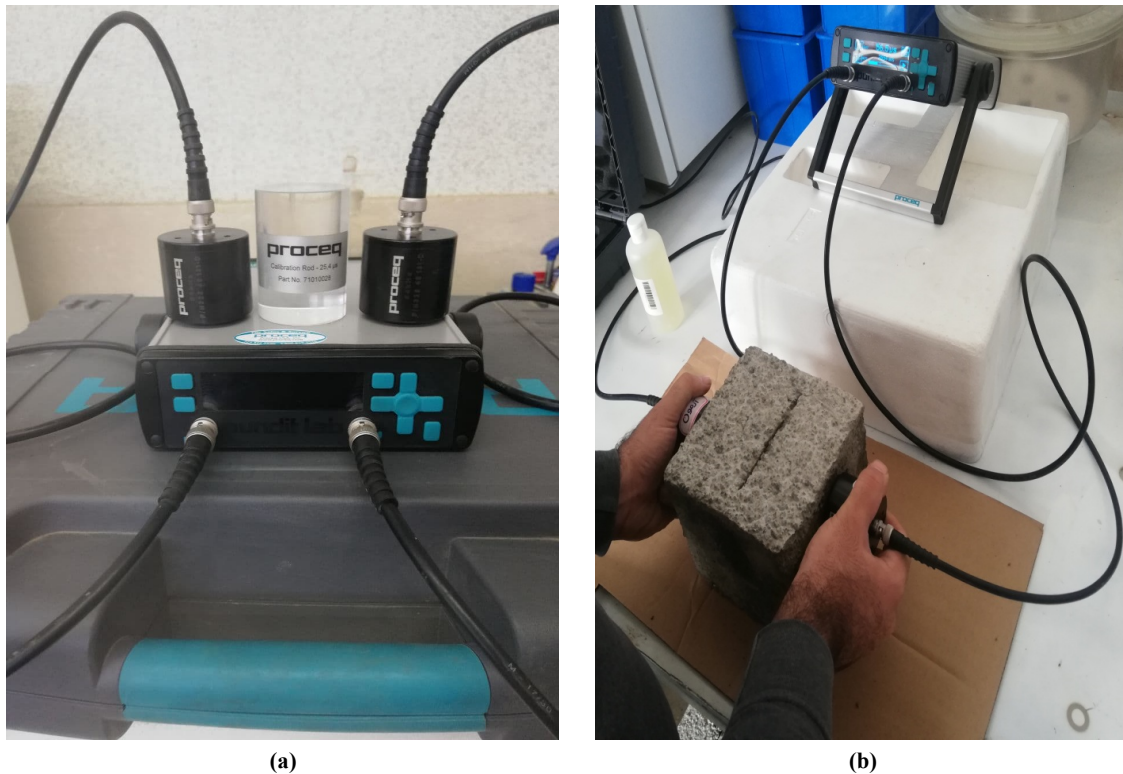


Figure 8. a) PUNDIT instrument used for measuring LWV, b) Measurement procedure for assessing LWV propagation through the prepared concrete samples.

### 3. Statistical analysis

#### 3.1. Impact of joint properties on LWV

Based on the tests discussed in the previous section, a suitable dataset was prepared for the necessary analyses. This section examines the effect of joint properties on the LWV. Relationships between the studied joint parameters—namely density, filling type, angle, aperture, and roughness—and LWV are illustrated in Figure 9a–e, respectively. As shown in these figures, joint density, joint roughness, and joint aperture all exhibit an inverse relation with LWV.

To investigate the effect of joint density on LWV, samples with 0 (no joints), 1, 2, 3, and 4 joints were tested. As demonstrated in Figure 9a, LWV decreases nonlinearly with an increasing number of joints. The LWV value decreases from 2720 m/s for the sample without joints to 480 m/s for the sample with 4 joints, representing a reduction rate of approximately 82%. Figure 9b indicates that gypsum and iron oxide filling materials yield the highest and lowest LWV values (2460 m/s and 1620 m/s, respectively). In contrast, silica, calcite, and clay filling materials result in moderate LWV values (1970 m/s, 1880 m/s, and 1865 m/s, respectively). Notably, the variation in

LWV across different filling materials is about 34%.

To assess the influence of joint angle on LWV, wave propagation through samples with joint angles of 30°, 45°, 60°, and 90° was investigated. A sinusoidal pattern emerges between LWV and joint angle, as illustrated in Figure 9c. As the joint angle increases from 30° to 45°, LWV rises from 1910 m/s to 1950 m/s. However, as the joint angle increases to 60°, LWV decreases to 1840 m/s, before rising again to 2050 m/s at a joint angle of 90°. The difference between the lower and upper limits of LWV across different joint angles is relatively small, with about a 10% variation.

As depicted in Figure 9d, LWV decreases nonlinearly with an increase in joint aperture. The LWV value drops from 2050 m/s for a joint aperture of 0.5 mm to 1045 m/s for a joint aperture of 2 mm, resulting in a reduction rate of 49%. Finally, Figure 9e demonstrates that LWV decreases nonlinearly as the joint roughness coefficient increases. Specifically, the LWV value declines from 2050 m/s for a smooth joint to 1590 m/s for a joint roughness coefficient of 14, representing a reduction rate of 22.5%.

Similar findings regarding the decrease in LWV with an increase in joint density [7, 19, 32–36], roughness [7, 22, 23, 37, 38, 40], and aperture [40,

41] have been reported by previous researchers. Conversely, the relationship between joint angle and LWV follows a sinusoidal pattern; joint angles of 90° and 60° correspond to the highest and lowest LWV values, respectively. It is noteworthy that earlier investigators [7, 34, 39] have also observed a similar trend in LWV variation with increasing

angle. Finally, the relationship concerning joint filling type indicates that gypsum results in the highest LWV value while iron oxide filling leads to the lowest. Meanwhile, calcite and clay fillings produce closely comparable LWV values that are slightly lower than those associated with silica filling.

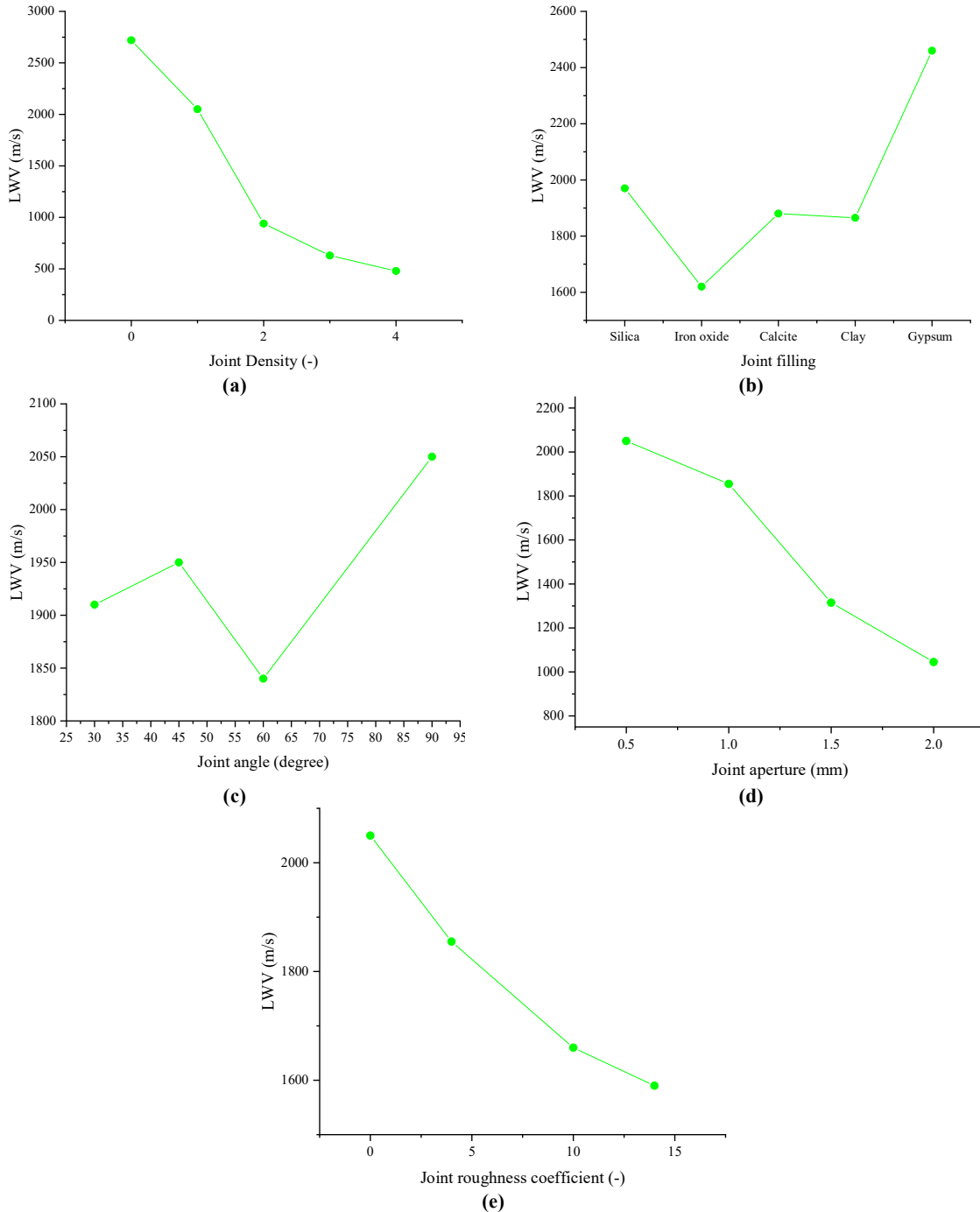


**Figure 9. Relationship of LWV with joint properties: a) Relationship of LWV with joint density, b) Relationship of LWV with joint filling, c) Relationship of LWV with joint angle, d) Relationship of LWV with the joint ape, e) Relationship of LWV with joint roughness coefficient.**

### 3.2. Development of optimum relations

To develop experimental-statistical equations that relate joint characteristics to the LWV, an analysis of variance (ANOVA) was employed. ANOVA is a widely used statistical techniques in various engineering disciplines. Five equations—linear, quadratic polynomial, logarithmic, exponential, and power relations—were independently established to describe the relationships between joint characteristics and LWV. The optimal equation for each case was selected based on three criteria: determination coefficient ( $R^2$ ), Fisher-test coefficient (F), and statistical significance (Sig.).

The ANOVA results presented in Table 1 identify the best-fitting equations between LWV and joint properties, which include density, angle, aperture, and roughness. As indicated, quadratic polynomial equations were found to provide the

best fit for all examined joint properties. Consequently, these optimal experimental-statistical equations are proposed in this study to estimate LWV based on specific joint characteristics. Figures 10a–d illustrate the optimal relationships between LWV and joint density ( $J_n$ ), joint angle ( $J_{an}$ ), joint aperture ( $J_{ap}$ ), and joint roughness ( $J_r$ ), respectively. As shown in these figures, LWV exhibits a non-linear inverse relationship with  $J_n$ ,  $J_{ap}$  and  $J_r$ . In contrast, there is a non-linear sinusoidal relationship between LWV and  $J_{ap}$ , as demonstrated in Figures 9e and 10d.

Based on the determination coefficient presented in Table 1 and Figures 10a–d, it can be concluded that LWV shows a strong correlation with joint roughness compared to other joint properties. Conversely, joint angle exhibits the weakest correlation with LWV among the studied joint properties.

**Table 1. Summary of ANOVA results for optimal equations between LWV and joint properties.**

Joint property	Optimal equation type	Equation	$R^2$	F	Sig.
$J_n$ (-)	Quadratic	$LWV=131.428J_n^2-1115.714J_n+2806.857$	0.977	43.043	0.023
$J_{an}$ (degree)	Quadratic	$LWV=0.11J_{an}^2-11.53J_{an}+2180$	0.694	1.139	0.05
$J_{ap}$ (mm)	Quadratic	$LWV=-75J_{ap}^2-523.5J_{ap}+2361.25$	0.971	16.744	0.016
$J_r$ (-)	Quadratic	$LWV=1.5625J_r^2-54.67672J_r+2049.61207$	0.99	33180.33	0.004

### 4. Results verification

As discussed in section 2.1, two new artificial samples were prepared to validate the proposed equations relating LWV to various joint properties. The values for each joint property entered were input into the suggested equations, and the resulting LWV values were compared with the actual experimental results. The outcomes of this comparative analysis are presented in Table 2. The table indicates that for a sample with five joints, the error is 13%, which falls within an acceptable range and supports the validity of the proposed equation. However, for the sample with six joints, the error is significantly higher and deviates considerably from the experimental result. This substantial error is attributed to the increased joint frequency relative to the sample length in this study. Specifically, having six joints in a 15 cm sample raises the frequency and the associated error, suggesting that the proposed equation is only applicable to samples with fewer than six joints.

Regarding joint angles, the error of  $15^\circ$  and  $75^\circ$  joint angles are 3% and 4%, respectively, both of which are acceptable. The predicted values closely align with the experimental results, demonstrating the reliability of the equation. For a joint aperture

of 2.5 mm, the error is 10%, which is also within a reasonable range. However, the error for a 3 mm aperture is significantly higher, as the value exceeds the typical range for natural joints. The proposed analytical model assumes a descending relationship that does not fully account for larger joint apertures; thus, the equation is valid for apertures smaller than 3 mm. The resulting errors for joint roughness values of 8–10 and 18–20 are 3% and 7%, respectively. These errors are acceptable and illustrate the equation's capability to predict LWV based on joint roughness. In conclusion, these verification results suggest that the proposed equations are reasonably valid and can serve as predictive tools for determining LWV values in jointed rocks under similar conditions.

In addition to the comparisons above, measured LWV values and predicted LWV values from all proposed equations (for eight samples) were compared and the obtained results are shown in Figure 11. This comparison is presented in terms of the  $R^2$  and root mean square error (RMSE). As illustrated in Figure 11, the achieved values of  $R^2$  and RMSE are 0.926 and 189.08 m/s. These results generally demonstrate the effectiveness of the proposed equations in predicting LWV.

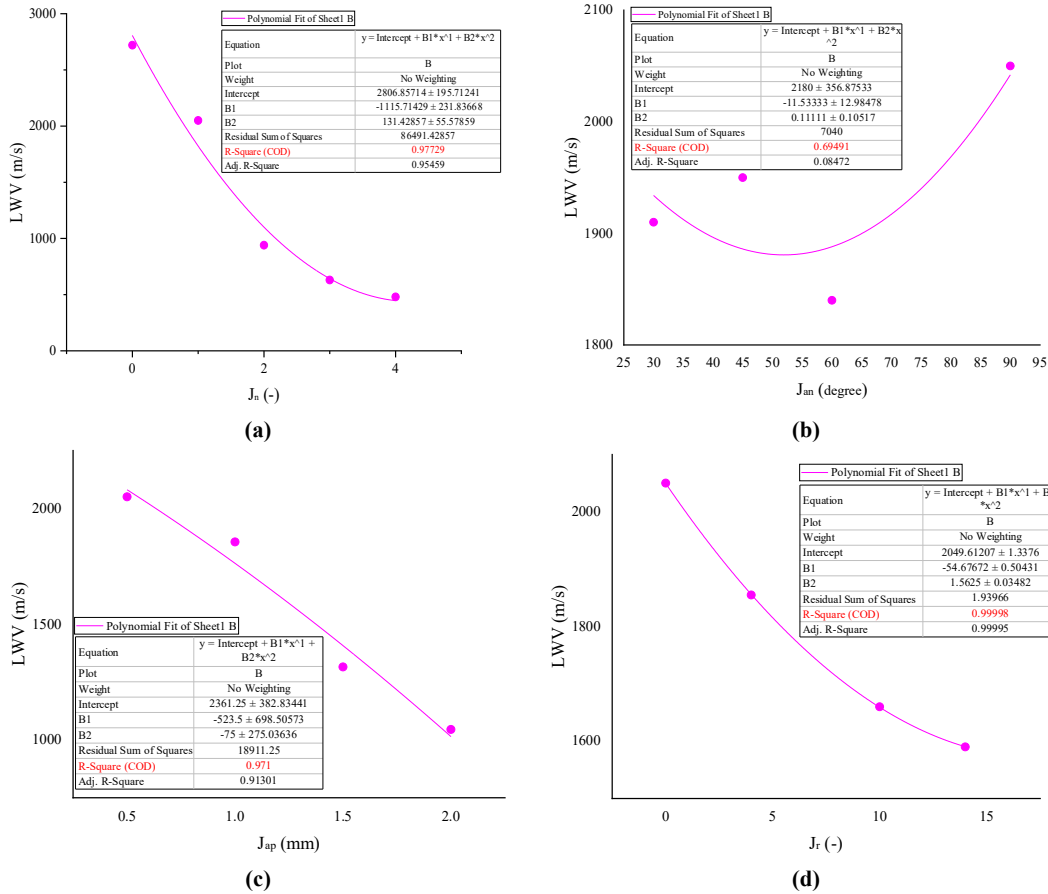


**Figure 10. Optimal relationships between LWV and joint properties: a) Optimum relation between LWV and joint density, b) Relationship between LWV and joint angle, c) Relationship between LWV and joint aperture, d) Relationship between LWV and joint roughness.**

**Table 2. Comparing the results of suggested equations with actual LWV values.**

Join properties	Input value	Actual LWV (m/s)	Predicted LWV (m/s)	Relative error (%)
J <sub>n</sub> (-)	5	450	511.7	13
	6	470	841.4	79
J <sub>an</sub> (degree)	15	2100	2031.9	3
	75	1850	1939.4	4
J <sub>ap</sub> (mm)	2.5	650	584.7	2.5
	3	450	117	74
J <sub>r</sub> (-)	8-10	1650	1712.6	3
	18-20	1460	1572.2	7

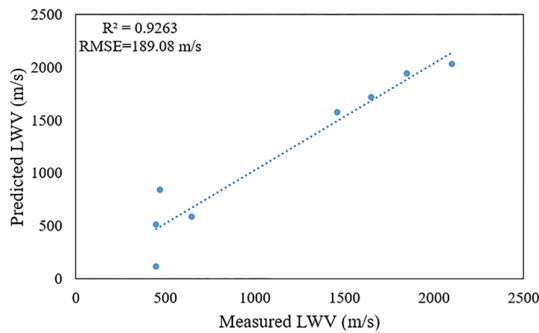


**Figure 11. Comparison between measured and predicted LWV values from the proposed equations for eight samples.**

### 5. Research benefits, limitations and recommendations

This study investigates the impact of key rock joint characteristics on LWV. The findings address the scarcity of laboratory data regarding wave behaviour in jointed rock masses under various conditions. By examining factors such as density, filling type, angle, aperture, and roughness, this research enhances our understanding of how these parameters influence LWV. The laboratory results support the development of theoretical and statistical models for wave propagation in jointed

rock masses, providing insights into wave behaviour across diverse conditions. These findings can facilitate preliminary evaluations and offer reliable constraints on wave propagation in jointed rock masses, which is crucial for understanding rock mass dynamics in engineering applications.

Furthermore, this study demonstrates that LWV can be estimated indirectly using derived equations based solely on specific joint properties, including density, angle, aperture, and roughness. The outcomes of this research may also assist in interpreting seismic data collected from underground sites and open-pit slopes, where joint characteristics play a vital role in analyzing rock mass stability. However, it is important to note that these findings must be generalized and extrapolated to field conditions, as laboratory standards for LWV testing differ from those applicable to field-scale data.

It is also essential to highlight that the experiments conducted in this study were performed under relaxed conditions, without confining pressure or water saturation. In contrast, natural rock joints and those encountered in practical engineering settings often exist under more complex environmental conditions involving confining stresses, temperature variations, and fluid pressures. For instance, the presence of fluids in joints can significantly change seismic velocities, complicating interpretations of rock mass behaviour. Therefore, accurately identifying and quantitatively assessing the effects of joint properties on wave propagation across in-situ rock masses will likely require additional datasets, including information on rock properties, fluid characteristics, pore attributes, and seismic data.

Moreover, further research is needed to explore jointed rock masses filled with other common natural minerals, such as illite and chlorite, to fully understand how mineralogical composition impacts wave propagation. This study primarily focused on the effects of LWV incidence on rock samples with simple joint structures. Future research should consider more complex joint arrangements, such as intersecting joints. Additionally, since shear wave velocity is frequently encountered in both natural and anthropogenic contexts, it is essential to investigate how joint characteristics influence shear wave velocity in future studies.

## 6. Conclusions

In this study, the effect of joint properties (i.e., density, filling type, angle, aperture, and roughness) on the propagation of LWV through artificially jointed rock samples was investigated. The key findings are as follows:

- A homogeneous mixture consisting of 75% sand, 15% cement, and 10%, produced an optimal artificial with maximum strength.
- Experimental results indicated that LWV has an inverse relationship with the joint density, aperture, and roughness, resulting in reductions of LWV by 82%, 22.5% and 49%, respectively.
- The relationship between joint angle and LWV was found to be sinusoidal: LWV increases from 30° to 45°, decreases from 45° to 60°, and increases from 60° to 90°. However, the variations in LWV across different joint angles was approximately 10%.
- Gypsum filling resulted in the highest LWV values, while iron oxide filling yielded the lowest. Calcite and clay fillings produced similar LWV values that were both lower than those associated with silica filling. The variation in LWV due to different filling materials was about 34%.
- Based on the experimental data and analysis of variance (ANOVA), quadratic polynomial relations were established as the best fit for LWV concerning joint density ( $R^2=0.977$ ), aperture ( $R^2=0.971$ ), angle ( $R^2=0.694$ ), and roughness ( $R^2=0.99$ ) parameters.
- Verification using laboratory samples demonstrated a low relative error (approximately 3%–13%), an acceptable RMSE of 189.08 m/s, and a high  $R^2$  value of 0.926, confirming the reliability of these relationships for determining LWV. However, these relationships are valid only for joint density less than 6 and joint aperture less than 3 mm, respectively.
- This research enhances our understanding of wave propagation through jointed rock masses with varying joint characteristics and filling materials, providing valuable theoretical insights for analyzing the dynamic behaviour and stability of rock masses containing structural planes.

## References

- [1]. Barton, N. (2006). Rock quality, seismic velocity, attenuation and anisotropy. Tylor & Francis e- Library, London, UK, 729 P.
- [2]. Bagher Shemirani, A., Haeri, Hadi., Sarfarazi, V., & Hedayat, A. (2017). A review paper about experimental

- investigations on failure behaviour of non-persistent joint. *Geomechanics and Engineering*, 13(4), 535–570.
- [3]. Sarfarazi, V., Haeri, H., Fatehi Marji, M., Saeedi, G., & Namdarmanesh, Amir. (2023). Investigation of Shear Properties of Open Non-persistent Latitudinal Discontinuities of Same Level. *Journal of Mining and Environment*, 14(4), 1361–1371.
- [4]. Haeri, H., Sarfarazi, V., Ebneabbasi, P., Nazari maram, A., Shahbazian, A., Fatehi Marji, M., & Mohamadi, A.R. (2020). XFEM and experimental simulation of failure mechanism of non-persistent joints in mortar under compression. *Construction and Building Materials*, 236, 117500.
- [5]. Siamaki, A., & Bakhshandeh Amnie, H. (2016). Numerical analysis of energy transmission through discontinuities and fillings in Kangir Dam. *Journal of Mining and Environment*, 7(2), 251–259.
- [6]. Fatemi Aghda, S.M., Kianpour, M., & Talkhablou, M. (2019). Efficiency of seismic wave velocity and electrical resistivity in estimation of limestone rock mass quality indices (Q, Q<sub>sr</sub>) (Case study: Asmari formation, SW Iran). *Journal of Mining and Environment*, 10(2), 529–541.
- [7]. Varma, M., Maji, V.B., & Boominathan, A. (2021). Influence of rock joints on longitudinal wave velocity using experimental and numerical techniques. *International Journal of Rock Mechanics and Mining Sciences*, 141, 104699.
- [8]. Walsh, J.B. (1966). Seismic attenuation in rock due to friction. *Journal of Geophysical Research*, 71(10), 2591–2600.
- [9]. Miller, R.K. (1977). An approximate method of analysis of the transmission of elastic waves through a frictional boundary. *Journal of Applied Mathematics*, 44(4), 652–656.
- [10]. Miller, R.K. (1978). The effect of boundary friction on the propagation of elastic waves. *Bulletin of the Seismological Society of America*, 68(4), 987–998.
- [11]. Schoenberg, M. (1980). Elastic wave behavior across linear slip interfaces. *Journal of the Acoustical Society of America*, 68, 1516–1521.
- [12]. Myer, L.R. (2000). Fractures as a collection of cracks. *International Journal of Rock Mechanics and Mining Sciences*, 37(1–2), 231–243.
- [13]. Cai, J.G., & Zhao, J. (2000). Effect of multiple parallel fractures on apparent attenuation of stress waves on rock masses. *International Journal of Rock Mechanics and Mining Sciences*, 37(4), 661–682.
- [14]. Perino, A., Zhu, J.B., Li, J.C., Barla, G., & Zhao, J. (2010). Theoretical methods for wave propagation across jointed rock masses. *Rock Mechanics and Rock Engineering*, 43(6), 799–809.
- [15]. Fan, L., Ma, G., & Li, J. (2012). Nonlinear viscoelastic medium equivalence for stress wave propagation in a jointed rock mass. *International Journal of Rock Mechanics and Mining Sciences*, 50, 11–18.
- [16]. Zou, Y., Li, J., He, L., Laloui, L., & Zhao, J. (2016). Wave propagation in the vicinities of the rock fractures under obliquely incident wave. *Rock Mechanics and Rock Engineering*, 49(5), 1789–1802.
- [17]. Ju, Y., Sudak, L., & Xie, H. (2007). Study on stress wave propagation in fractured rocks with fractal joint surfaces. *International Journal of Solids and Structures*, 44(13), 4256–4271.
- [18]. Zhao, X.B., Zhao, J., Cai, J.G., & Hefny, A.M. (2008). UDEC modelling on wave propagation across fractured rock masses. *Computers and Geotechnics*, 35(1), 97–104.
- [19]. Cha, M., Cho, G.C., & Santamaria, J.C. (2009). Long-wavelength P-wave and S-wave propagation in jointed rock masses. *Geophysics*, 74(5), E205–E214.
- [20]. Mollhoff, M., Bean, C.J., & Meredith, P.G. (2010). Rock fracture compliance derived from time delays of elastic waves. *Geophysical Prospecting*, 58(6), 1111–1121.
- [21]. Li, W., & Pyrak-Nolte, L.J. (2010). Seismic wave propagation in fractured carbonate rock. In: *Proceedings of the Project Review, Geo-Mathematical Imaging Group (Purdue University, West Lafayette IN)*, Vol. 1, pp. 211–220.
- [22]. Mohd-Nordin, M.M., Song, K., Cho, G., & Mohamed, Z. (2014). Long wavelength elastic wave propagation across naturally fractured rock masses. *Rock Mechanics and Rock Engineering*, 47(2), 561–573.
- [23]. Huang, X., Qi, S., Guo, S., & Dong, W. (2014). Experimental study of ultrasonic waves propagating through a rock mass with a single joint and multiple parallel joints. *Rock Mechanics and Rock Engineering*, 47(2), 549–559.
- [24]. Sebastian, R., & Sitharam, T.G. (2014). Transmission of Elastic waves through a frictional boundary. *International Journal of Rock Mechanics and Mining Sciences*, 66(4), 84–90.
- [25]. Sebastian, R., & Sitharam, T.G. (2015). Long-wavelength propagation of waves in jointed rocks-Study using resonant column experiments and model material. *Geomechanics and Geoengineering*, 11(4), 281–296.
- [26]. Wu, W., Li, H., & Zhao, J. (2015). Dynamic response of non-welded and welded rock fractures and implications for P wave attenuation in a rock mass. *International Journal of Rock Mechanics and Mining Sciences*, 77, 174–181.
- [27]. Wu, W., Li, H., Zhao, J. (2015). Rock of filling material in a P wave interaction with a rock fracture. *Engineering Geology*, 172, 77–84.

- [28]. Zhao, J., Cai, J.G., Zhao, X.B., & Li, H.B. (2006). Experimental study of ultrasonic wave attenuation across parallel fractures. *Geomechanics and Geoengineering*, 1(2), 87–103.
- [29]. Resende, R. (2010). An Investigation of Stress Wave Propagation through Rock Joints and Rock Masses. PhD Thesis, Porto University, Portugal.
- [30]. Eitzenberger, A. (2012). Wave Propagation in Rock and the Influence of Discontinuities. PhD Thesis, Luleå University of Technology, Sweden.
- [31]. Sebastian, R., & Sitharam, T.G. (2016). Transformations of obliquely striking waves at a rock joint: numerical simulations. *International Journal of Geomechanics*, 16(3), 04015079.
- [32]. Kahraman, S. (2001). A Correlation between P-Wave Velocity, Number of Joints and Schmidt Hammer Rebound Number. *International Journal of Rock Mechanics and Mining Sciences*, 38(5), 729–733.
- [33]. Altindag, R., & Guney, A. (2005). Evaluation of the Relationships between P-wave Velocity (LWV) and Joint Density (J). In: *The 19th International Mining Congress and Fair of Turkey (IMCET2005)*, Izmir Turkey, pp. 101–106.
- [34]. El Azhari, H., & El Amrani El Hassan, I.E. (2013). Effect of the Number and Orientation of Fractures on the P-Wave Velocity Diminution: Application on the Building Stones of the Rabat Area (Morocco). *Geomaterials*, 3(3), 34584.
- [35]. Saroglou, C.H., & Kallimogiannis, V. (2017). Fracturing Process and Effect of Fracturing Degree on Wave Velocity of a Crystalline Rock. *Journal of Rock Mechanics and Geotechnical Engineering*, 9(5), 797–806.
- [36]. Liu, Y., Lu, C.P., Liu, B., Zhang, H., & Wang, H.Y. (2019). Experimental and Field Investigations on Seismic Response of Joints and Beddings in Rocks. *Ultrasonics*, 97(4), 46–56.
- [37]. Kahraman, S. (2002). Effect of Fracture Roughness on P Wave Velocity. *Engineering Geology*, 63(3–4), 347–350.
- [38]. Li, Y., & Zhu, Z. (2012). Study on the Velocity of P Waves across a Single Joint based on Fractal and Damage Theory. *Engineering Geology*, 151, 82–88.
- [39]. Varma, M., Maji, V.B., & Boominathan, A. (2017). A Study on Ultrasonic Wave Propagation Across Fractures in Jointed Rocks. In: *51st U.S. Rock Mechanics/Geomechanics Symposium*, San Francisco, California, USA, ARMA–2017–0483.
- [40]. Huang, X., Qi, S., Williams, A., Zou, Y., & Zheng, B. (2015). Numerical Simulation of Stress Wave Propagating through Filled Joints by Particle Model. *International Journal of Solids and Structures*, 69–70, 23–33.
- [41]. Yang, H., Duan, H.F., & Zhu, J.B. (2019). Ultrasonic P-wave Propagation through Water-filled rock joint: An experimental investigation. *Journal of Applied Geophysics*, 169, 1–14.
- [42]. Abbas, H.A., Zainab, M., & Mohd-Nordin, M.M. (2022). Characterization of the Body Wave Anisotropy of an Interbedded Sandstone-Shale at Multi Orientations and Interlayer Ratios. *Geotechnical and Geological Engineering*, 40(7), 3413–3429.
- [43]. Fan, Z., Zhang, J., Xu, H., & Wang, X. (2022). Transmission and application of a P-wave across joints based on a modified  $g-\lambda$  model. *International Journal of Rock Mechanics and Mining Sciences*, 150, 104991.
- [44]. Tartoussi, N., Lataste, J.F., Rivard, P., & Barbosa, N.D. (2023). Effects of a filled discontinuity in a rock mass on transmission losses of compressional and shear wave of full-waveform sonic log data. *Journal of Applied Geophysics*, 217(53), 105179.
- [45]. Yang, H., Duan, H.F., & Zhu, J. (2023). Experimental study on the role of clay mineral and water saturation in ultrasonic P-wave behaviours across individual filled rock joints. *International Journal of Rock Mechanics and Mining Sciences*, 168, 105393.
- [46]. Hu, H., Yang, L., Feng, C., Zhu, X., Zhou, J., & Liu, X. (2024). Development of BB model and investigation of P-wave propagation across jointed rock masses using CDEM. *Computers and Geotechnics*, 165, 105910.
- [47]. Kaixing, W., Bin, W., Yishan, P., Khmelinin, A.P., & Chanyshv, A.I. (2024). Experimental Investigation of Block Fracture Influence on P-Wave Propagation in Block Rock Mass. *Journal of Mining Sciences*, 60(2), 210–219.
- [48]. Ramamurthy, T., & Arora, V.K. (1994). Strength Predictions for Jointed Rocks in Confined and Unconfined States. *International Journal of Rock Mechanics and Mining Sciences & Geomechanics Abstracts*, 31(1), 9–22.
- [49]. Sebastian, R. (2015). Elastic Wave Propagation and Evaluation of Low Strain Dynamic Properties in Jointed Rocks. PhD Thesis, Indian Institute of Sciences, Bangalore, India.
- [50]. Barton, N., & Choubey, V. (1977). The Shear Strength of Rock Joints in Theory and Practice. *Rock Mechanics*, 10(1), 1–54.
- [51]. Rezaei, M., Koureh Davoodi, P., & Najmoddini, I. (2019). Studying the Correlation of Rock Properties with P-wave Velocity Index in Dry and Saturated Conditions. *Journal of Applied Geophysics*, 169, 49–57.
- [52]. Rezaei, M. (2020). Feasibility of novel techniques to predict the elastic modulus of rocks based on the laboratory data. *International Journal of Geotechnical Engineering*, 14(1), 25–34.

- [53]. Rezaei, M., & Koureh Davoodi, P. (2021). Determination of Relationships between the Shear Wave Velocity and Physicomechanical Properties of Rock. *International Journal of Mining and Geo-Engineering*, 51(1), 63–70.
- [54]. Seyed Mousavi, S.Z., & Rezaei, M. (2023). Assessing the long-term durability and degradation of rocks under freezingthawing cycles. *Geomechanics and Engineering*, 34(1), 51–67.
- [55]. Rezaei, M., & Nyazyran, N. (2023). Assessment of Effect of Rock Properties on Horizontal Drilling Rate in Marble Quarry Mining: Field and Experimental Studies. *Journal of Mining and Environment*, 14(1), 321–339.
- [56]. Wang, Y., Rezaei, M., Abdullah, R.A., & Hasanipanah, M. (2023). Developing Two Hybrid Algorithms for Predicting the Elastic Modulus of Intact Rocks. *Sustainability*, 15, 4230.
- [57]. Rezaei, M., & Esmaeili, K. (2024). The Anisotropy of Rock Drilling in Marble Quarry Mining Based on the Relationship between Vertical and Horizontal Drilling Rates. *International Journal of Geomechanics*, 24(10), 04024236.
- [58]. ISRM. (1978). Suggested Method for Determining Sound Velocity *International Journal of Rock Mechanics and Mining Sciences & Geomechanics Abstracts*, 15(2), 53–58.

## بهبود تعیین سرعت موج طولی با در نظر گرفتن تأثیر خصوصیات درزه در نمونه‌های سنگ مصنوعی

محمد رضائی<sup>۱\*</sup>، سید پوریا حسینی<sup>۱</sup>، دانیال جاهد ارمانی<sup>۲</sup> و منوج کاندلوال<sup>۳</sup>

۱- گروه مهندسی معدن، دانشکده مهندسی، دانشگاه کردستان، ایران

۲- دانشکده مهندسی عمران و محیط زیست، دانشگاه فناوری سیدنی، استرالیا

۳- موسسه نوآوری، علم و پایداری، دانشگاه فدراسیون استرالیا، استرالیا

ارسال ۲۰۲۴/۱۰/۲۴، پذیرش ۲۰۲۴/۱۲/۱۹

\* نویسنده مسئول مکاتبات: m.rezaei@uok.ac.ir

### چکیده:

این مقاله یک مطالعه آزمایشگاهی-آماری را ارائه می‌کند که در آن، تأثیر پنج ویژگی درزه شامل تراکم، نوع ماده پرکننده، زاویه، دهانه و زبری بر سرعت موج طولی نمونه‌های بتنی مورد بررسی قرار گرفته است. بدین منظور، هر کدام از پنج ویژگی فوق‌الذکر به گروه‌های مجزا با بازه‌های مخصوص طبقه‌بندی شدند. نمونه‌های بتنی در ابعاد ۱۵×۱۵×۱۵ سانتی‌متر بر اساس ترکیب بهینه ۷۵٪ ماسه، ۱۵٪ سیمان و ۱۰٪ آب در آزمایشگاه آماده‌سازی گردید. سپس، مقادیر سرعت موج طولی این نمونه‌ها اندازه‌گیری شد. نتایج تجربی نشان داد که تراکم، زبری و دهانه درزه دارای رابطه معکوس با سرعت موج طولی هستند که به ترتیب منجر به کاهش ۸۲٪، ۲۲/۵٪ و ۴۹٪ سرعت موج طولی می‌شوند. علاوه بر این، یک رابطه تقریباً سینوسی بین سرعت موج طولی و زاویه درزه اثبات گردید که منجر به تغییر حدوداً ۱۰٪ در مقادیر سرعت موج طولی برای زوایای مختلف درزه می‌شود. برای ارزیابی اثر ماده پرکننده درزه بر سرعت موج طولی، از مواد پرکننده مختلف، از جمله اکسید آهن، کلسیت، سیلیس، خاک رس و گچ استفاده شد که باعث ۳۴٪ تغییر در مقادیر سرعت موج طولی می‌گردند. همچنین، مشخص شد که مواد پرکننده گچ و اکسید آهن به ترتیب منجر به بیش‌ترین و کم‌ترین مقدار سرعت موج طولی می‌شوند. بعلاوه، تجزیه و تحلیل واریانس نتایج آزمایشگاهی نشان داد که معادله چند جمله‌ای درجه دوم بهترین رابطه بین سرعت موج طولی و هر کدام از خصوصیات درزه با مقادیر ضریب تعیین از ۰/۶۹۴ تا ۰/۹۹ است. در نهایت، مطالعه اعتبارسنجی با استفاده از «نمونه‌های راستی‌آزمایی» دقت قابل قبول معادلات پیشنهادی با مینیمم خطای نسبی از ۳٪ تا ۱۳٪، مقدار پایین ریشه میانگین مربعات خطا (۱۸۹/۰۸ متر بر ثانیه)، و مقدار ضریب تعیین بالا (۰/۹۲۶) را نشان داد. این تحقیق شناخت نحوه انتشار امواج در داخل توده‌سنگ‌های درزدار با خصوصیات مختلف درزه را افزایش داده و یک بینش نظری برای شناخت بیشتر توده‌سنگ و تجزیه و تحلیل پایداری دینامیکی آن را فراهم می‌کند.

**کلمات کلیدی:** توده‌سنگ، درزه، سرعت موج طولی، مطالعه آزمایشگاهی، تحلیل آماری.